IEEE Access
Multidisciplinary ⋮ Rapid Review ⋮ Open Access Journal

Received 7 March 2023, accepted 26 March 2023, date of publication 7 April 2023, date of current version 19 April 2023.

Digital Object Identifier 10.1109/ACCESS.2023.3264612

RESEARCH ARTICLE

A Novel Conformal Quasi-Yagi Antenna With Offset Feed for High Directional 300GHz Applications

ANVESHKUMAR NELLA[1], (Member, IEEE), VIGNESWARAN DHASARATHAN[2], JAN KŘÍŽ[3], TATHABABU ADDEPALLI[4], ŠTĚPÁN HUBÁLOVSKÝ[5], AND MANISH SHARMA[6], (Senior Member, IEEE)

[1]School of Electrical and Electronics Engineering, VIT Bhopal University, Bhopal, Madhya Pradesh 466114, India
[2]Department of Applied Cybernetics, Faculty of Science, University of Hradec Králové, 50003 Hradec Králové, Czech Republic
[3]Department of Physics, Faculty of Science, University of Hradec Králové, 50003 Hradec Králové, Czech Republic
[4]Department of Electronics and Communication Engineering, Aditya Engineering College, Surampalem 533437, India
[5]Department of Applied Cybernetics, Faculty of Science, University of Hradec Králové, 50003 Hradec Králové, Czech Republic
[6]Chitkara University Institute of Engineering and Technology, Chitkara University, Rajpura, Punjab 140401, India

Corresponding author: Manish Sharma (manishengineer1978@gmail.com)

This work was supported in part by the Project of Excellence, Faculty of Science, University of Hradec Králové, Czech Republic, under Grant 2214/2023-2024.

ABSTRACT This communication reports a conformal offset feed Quasi-Yagi antenna at 300 GHz for high-directional applications. A novel offset feed mechanism is adopted to obtain directional behavior from a conventional planar structure. The proposed antenna is designed on a Silicon-dioxide (SiO_2) dielectric substrate having a permittivity (ε_r) of 4 and a height of 60μm. A gold material of thickness 5μm is used as a conducting metal in the top and bottom layers. This antenna consists of an offset feed patch, partial ground as a reflector, and three director elements forming a Quasi-Yagi antenna. This conformal structure operates from 270 GHz to 333 GHz and provides a peak gain of 8.62dBi at 300 GHz in the end-fire direction. An analysis of different metals and parametric variation in metal thickness, substrate thickness, patch length, and width is also reported for a better understanding of the evolution of the proposed structure. A lumped equivalent circuit is also developed for the proposed structure to study its transmission line model. A good agreement is also noted between the EM simulation (HFSS, CST) and circuit simulation (ADS).

INDEX TERMS Conformal patch, director, offset-feed, Quasi-Yagi reflector, SiO_2, THz antenna.

I. INTRODUCTION

In modern communication systems, the THz range (100 GHz to 10 THz) occupies a vital place due to the increase in demand for higher data transmission rates [1]. The applications of communication may include remote sensing, biological detection, chip-to-chip communication or on-chip communication, and body area networks (BAN) [1], [2], [3], [4], [5]. Communication at the THz range has more challenges such as absorption by molecules in the atmosphere, and the signal can travel line-of-sight (LOS) or Non-LOS. For a lower band of THz, 0.1 THz to 1.5 THz is the probable wavelength of absorption in THz frequencies. However, the THz antenna should possess a high directivity to mitigate the constraint of distance traveled irrespective of path loss suffered by the signal at the THz range. It is also expected that the use of wireless networks will approximately target 75 Billion users by the end of 2025 and hence, the potential for research work arises. Literature study presents several millimeters and THz antennas for advanced wireless communication applications [1], [2], [3], [4], [5], [6], [7], [8], [9], [10], [11], [12], [13], [14], [15], [16], [17], [18], [19], [20], [21]. A photonic crystal substrate is used with the shape of the patch being trapezoidal targeting a THz bandwidth between 0.88 THz to 1.62 THz [1]. Rogers RO3003 substrate is used in the design of the proposed antenna, which possesses

The associate editor coordinating the review of this manuscript and approving it for publication was Saroj Tripathi.

$\varepsilon_r/\tan\phi = 3.00/0.0013$ (where ϕ is the angle between imaginary and real permittivity). In this work, the elimination of surface waves at those frequencies is achieved by creating hexagonal-shaped-photonic crystals. A 60 GHz high-frequency antenna is reported [2] with an overall volume of $3.5 \times 3.0 \times 0.42$ mm^3 and Low-Temperature Co-fired Ceramics (LTCC) substrate is employed. A gap-coupling technique is adopted to achieve the resonant frequency at 60 GHz. Photonic-band-gap structures are used in designing the microstrip patch antenna, providing a maximum gain of 7.703 dBi at 1.40 THz, which increases the operating range from 0.60 THz to 1.60 THz [3]. Using graphene material, the patch can overcome scattering losses and has the capability of sustaining electromagnetic propagation at the THz band. The purpose of the graphene antenna discussed in [4] is to provide a tremendous bandwidth of 5.4 GHz. A THz antenna with micron-level metal etching on a substrate of $423 \times 345 \times 6.5$ μm^3 is performed and dual-spaced multiple SSRs are obtained to provide a very high-frequency bandwidth from 274.10 GHz to 295.60 GHz [5]. A beam switching array, with an individual array consisting of 16-patches offers beam steering between $-32°$ to $+34°$ with a resonant frequency at 61 GHz [6-8, 10]. A THz antenna, providing an efficiency of 93% with a maximum gain of 5.60 dBi, operating between 0.258 THz to 0.385 THz is circularly polarized, where slots are used in the linear strip antenna [9]. A 16-element array, providing a peak gain of 15 dBi, achieves resonance at 77 GHz, which is useful for automotive applications [11]. A fractal antenna, with dimensions $800 \times 600 \times 81.29$ μm^3, provides a bandwidth of 9 THz (0.30 THz to 9.30 THz). This antenna consists of two slotted elliptical patches with a partial ground plane [12], [14], [19], [20]. A single elliptical patch with a partial ground produces a THz bandwidth from 0.46 THz to 5.46 THz and a maximum gain of 12.0 dBi [16]. A Koch-Snowflake fractal MIMO antenna, with overall dimensions of 820×1000 μm^2, provides an operational bandwidth from 1.06 THz to 14.20 THz and also offers a good diversity performance [17], [18]. A high gain antenna for 300 GHz with a Fabry-Perot cavity, providing the bandwidth for 6G wireless applications, is embedded with seven metallic structures and is integrated with horn-element and frequency-selective surfaces [21]. Literature [22], [23] also reports a study on lumped equivalent models. A super-wideband MIMO antenna produces THz bandwidth from 0.72 THz to 10.0THz with an isolation of more than 20 dB [24]. A graphene-based 2-port MIMO antenna offers THz bandwidth from 1.76 THz to 1.86 THz with isolation <25.0 dB [25]. A four-port antenna with a dimension of 45μm $\times$ 45μm generates a bandwidth range of 2.38 - 11.18 THz and utilizes a self-similar elliptic structure with a polyamide substrate [26]. A tunable-enhanced isolation MIMO antenna is reported [27], which provides a bandwidth range of 5.68 - 6.51THz and achieves ECC = 4.818×10^{-7}. A frequency span of 1.0 - 20.0 THz in a two-port antenna provides maximum isolation of 38dB with $S_{11} = -50.85$dB [28].

In recent times, advanced wireless communication systems require compact, cost-effective, high-gain, portable, conformal, and well-performing antennas. The motivation behind our work in this article is to design a novel offset feed conformal THz antenna at 300 GHz operating in the 270 to 333 GHz band for THz wireless systems. A peak gain of 8.62 dBi at 300 GHz in the end-fire direction is noted. This work is designed with three antennas noted as Antenna A (Fig. 2), Antenna B (Fig. 3), and Antenna C (Fig. 4) to obtain the required conformal antenna (Fig. 5). This work accomplishes novelty by adopting an offset feed mechanism to obtain directional behavior from a conventional planar structure. The proposed directional antenna can be useful for various THz applications like 6G, THz Imaging, Spectroscopy, digital holography, and Ptychography. The 6G application characteristics will include features such as full satellite integration, full connectivity to an autonomous vehicle, etc. The THz antenna will support the transfer of information using the five human senses where neurological processes through sensory integration will be established and will transfer the data acquired from the five senses. As reported in, the THz imaging system which has developed very recently finds applications in imaging systems utilizing THz pulsed and continuous-wave imaging. THz antennas are also useful in THz Spectroscopy for cell detection and bacterial identification. Also, utilizing THz pulsed Spectroscopy, cancer detection is possible by identifying characteristics of cancer spectral lines.

The rest of the paper is organized as follows. Section II presents a discussion of different design steps followed to obtain the proposed offset feed conformal structure at 300 GHz. Section III reports a parametric variation on various patch and substrate dimensions, a study on different metals, and a discussion of results. Section IV performs the existing work comparison with the proposed work. Section V concludes the paper.

II. EVOLUTION OF THE PROPOSED THz ANTENNA

Fig. 1 depicts the evolution of the proposed work in three iterations, which later are converted to a highly directional antenna by following several other steps. Fig. 1(a) shows a conventional rectangular patch printed on one plane and a full ground on the opposite plane. A SiO_2 dielectric substrate, with a relative permittivity of $\varepsilon_r = 4$ is adopted. The rectangular patch dimensions are calculated by using the following equations as given below:

$$W_{patch} = \frac{C_o}{2f_o\sqrt{\frac{\varepsilon_s+1}{2}}} \tag{1}$$

$$\varepsilon_{eff.} = \frac{\varepsilon_s+1}{2} + \frac{\varepsilon_s-1}{2}\left[\frac{1}{\sqrt{1+12\frac{h_{sub}}{W_m}}}\right] \tag{2}$$

$$L_{patch} = \frac{C_o}{2f_0\sqrt{\varepsilon_{eff.}}} - 0.824h_{sub} \times \left(\frac{(\varepsilon_{eff.}+0.3)\left(\frac{W_m}{h_{sub}}+0.264\right)}{(\varepsilon_{eff.}-0.258)\left(\frac{W_m}{h_{sub}}+0.8\right)}\right) \tag{3}$$

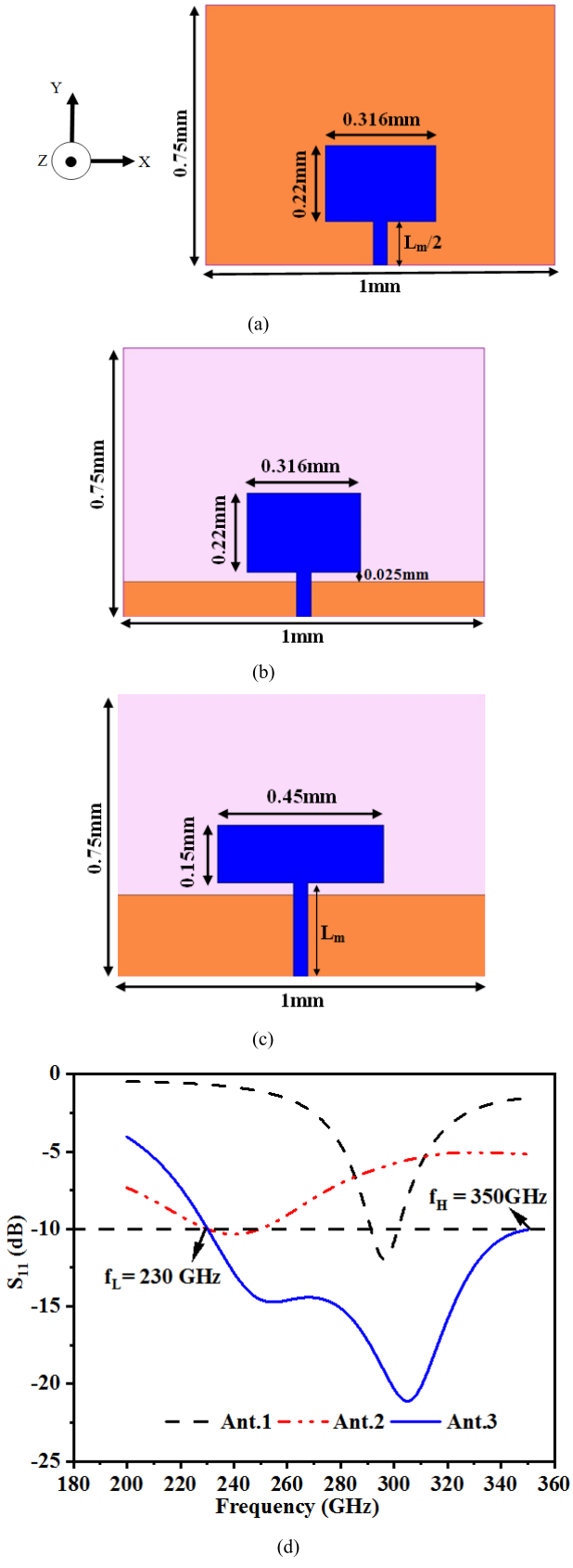

FIGURE 1. Initial Antenna Evolution (a) Ant. 1 (b) Ant. 2 (c) Ant. 3 (d) S_{11} result (Ant. 1–Ant. 3).

where W_{patch} and L_{patch} are the width and length of the rectangular radiating patch, ε_{eff} is the effective permittivity of the substrate. For a selected frequency of 300 GHz, the calculated patch length and width are 0.22mm and 0.316mm, respectively as shown in Fig. 1(a). This configuration produces a resonance at 296 GHz with poor impedance matching of S_{11} as −12dB shown in Fig. 1(d). Moreover, it is well known that the radiation pattern is not directional and normal to the antenna. Hence, to obtain a directional pattern by adopting a monopole structure and for better impedance matching, a partial ground is employed as shown in Fig. 1(b).

However, this structure resonates at 240 GHz. So, Fig. 1(c) is designed to meet the requirements in terms of impedance matching and directional properties. Fig. 1(c), with a new patch dimension of 0.45mm × 0.15mm, produces bandwidth ranging from f_L = 230GHz to f_H = 350GHz with the maximum matching of S_{11} = −21.12dB at 305 GHz as noted from Fig. 1(d). Now, to obtain the proposed conformal THz antenna configuration at 300 GHz with high directional properties, steps shown in Figs. 2 - 5 are performed. Fig. 2(a) and (b) show a transparent and perspective top view of the antenna.

The optimized dimensions are shown in Table 1 where the symbols are defined in Fig. 2 (a and b). A rectangular patch of dimension $P_L \times P_W$ μm^2 is connected to a 50 Ω microstrip feed-line with dimensions $W_m \times L_m$ μm^2. The ground plane printed on the opposite plane of the patch occupies a space of $W_g \times W_{SUB}$ μm^2. A gap (g) between the patch and ground is maintained with an optimum value of 33.50 μm for matching the impedance. Additionally, three identical metallic parasitic patches with dimensions $W_1 \times L_1$ μm^2 are also placed on the plane of the patch to accomplish directional characteristics.

TABLE 1. Optimized dimensions of antenna A.

Par.	Size (µm)	Par.	Size (µm)	Par.	Size (µm)
L_{SUB}	1350.0	W_m	40.0	d_1	200.0
W_{SUB}	1000.0	W_g	216.50	d_2	175.0
h_{SUB}	60.0	g	33.50	L_1	75.0
L_m	250.0	P_L	150.0	W_1	250.0
d	200.0	P_W	450.0	d_3	200.0

Fig. 2(c) shows the S-parameter graph that covers an impedance bandwidth from 231.28 GHz to 354.62 GHz with a resonating frequency at 300 GHz and S_{11} = −19.0 dB. This shows very poor matching of impedance due to the symmetrical structure. Moreover, Fig. 2(d) shows the 3D radiation suggesting that the radiation pattern does not meet the directional characteristics along $\phi = 90°$. The pattern is neither omnidirectional nor directional. It is required to radiate the signals in one direction with minimum back and side-lobe levels. To overcome the demerits such as poor impedance bandwidth and to achieve a high directional pattern,

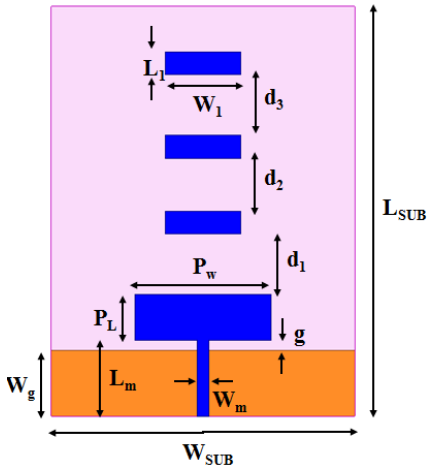

(a)

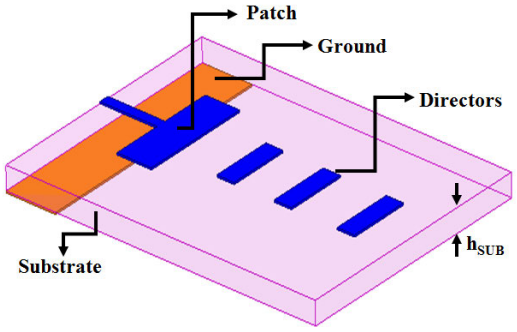

(b)

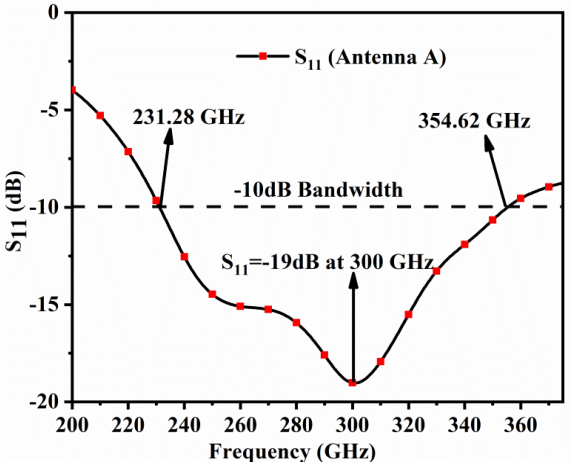

(c)

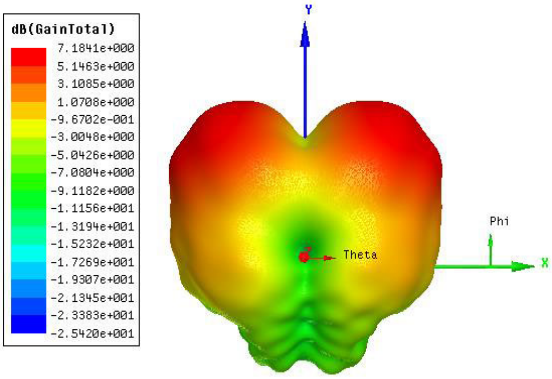

(d)

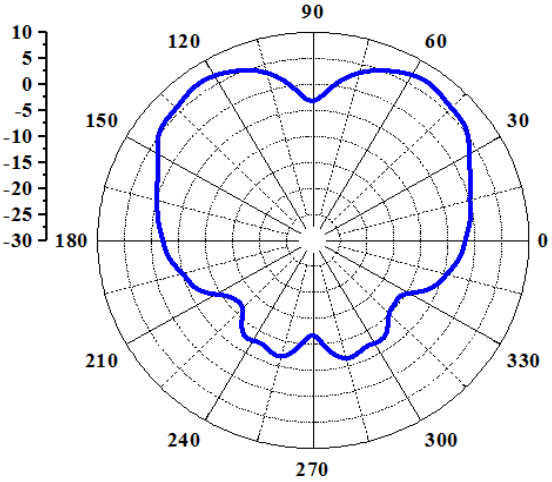

(e)

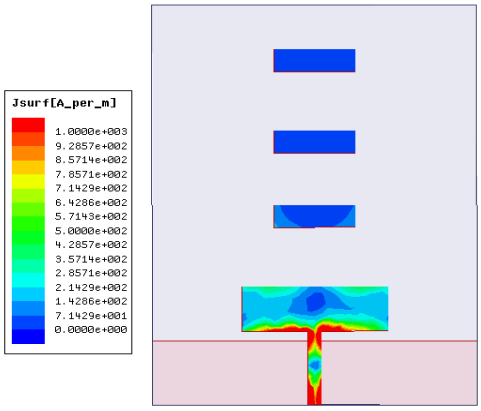

(f)

FIGURE 2. The initial design (Antenna A) (a) Transparent view with optimized dimensions (b) 3-D view (c) S_{11} (reflection coefficient) (dB) (d)-(f) 3D radiation pattern, XY-plane 2D pattern, surface current distribution at 300 GHz.

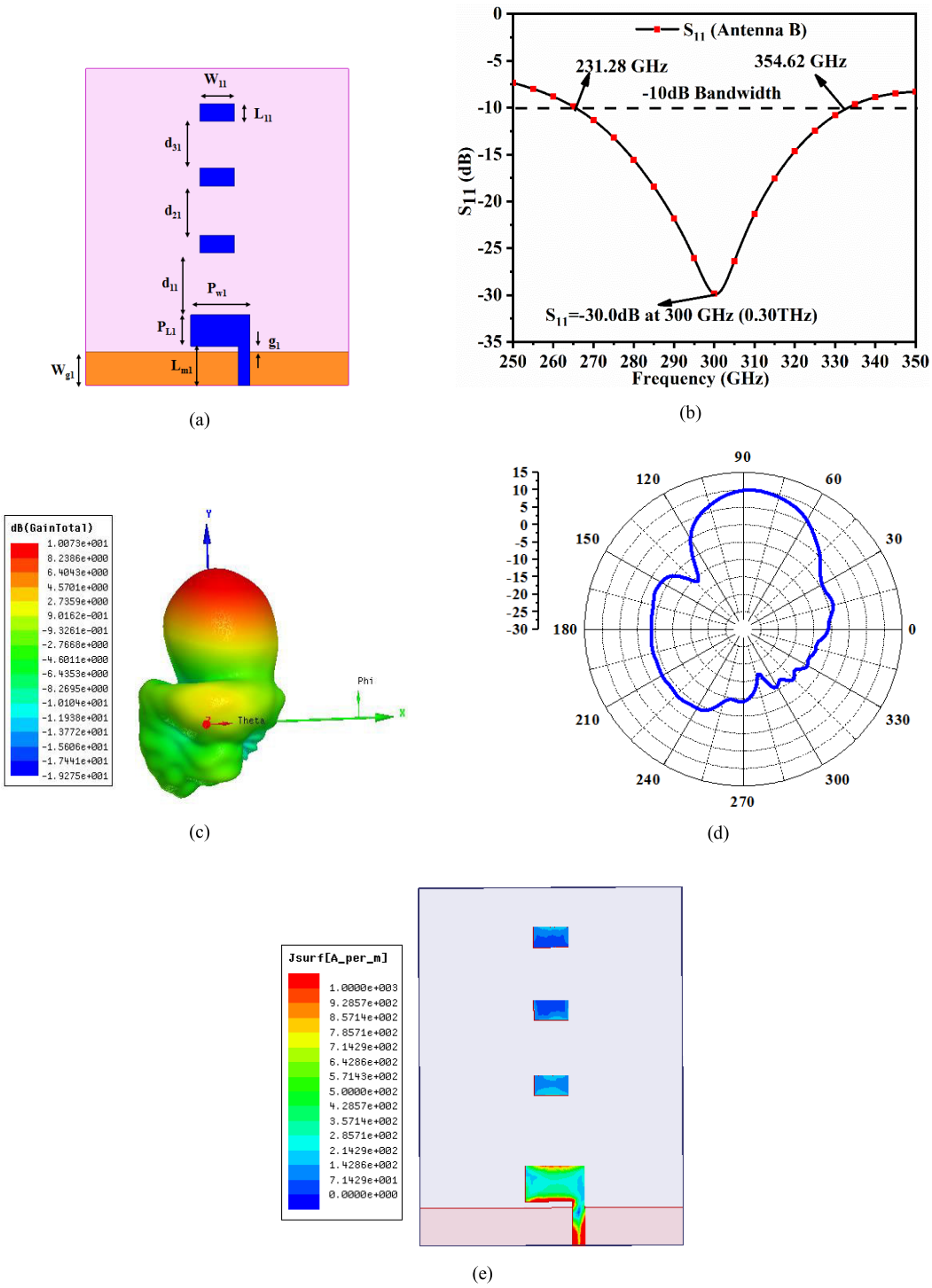

FIGURE 3. Second design (Antenna B) (a) Transparent view with optimized dimensions (b) S_{11} (dB) (c)-(e) 3D radiation pattern, XY-plane 2D pattern, surface current distribution at 300 GHz.

Antenna A, shown in Fig. 2(a), is modified with offset feed as shown in Fig. 3(a). The optimized values of the dimensions for Antenna B are tabulated in Table 2. As per the observations, Fig. 3(a) shows the asymmetric feed connected to the patch of dimension $P_{W1} \times P_{L1}$ μm^2 and parasitic patches of dimension $W_{11} \times L_{11}$ μm^2 with inter-spacing of d_{11}, d_{21}, and d_{31} respectively. On the opposite plane, the optimized ground of dimension $W_{g1} \times W_{SUB}$ μm^2 is printed with a gap

between the patch and ground as $g_1 = 22.75\ \mu$m. Antenna B provides -10.0 dB impedance bandwidth from 231.28 GHz to 354.62 GHz with a resonating frequency of 300 GHz and a corresponding $S_{11} = -30.0$ dB as shown in Fig. 3(b). From this design, it can be noted that the directional behavior of the antenna along the end-fire direction ($\phi =$ around 90° but not exactly) is achieved using an offset feed mechanism. This version of the modified antenna with asymmetric feed achieves the main lobe directed towards around 90° concerning frequency centered at 300 GHz. The final version of the planar patch antenna, shown in Fig. 4(a), is etched with a rectangular slot, and the width of the strip is reduced to $P_1\ \mu$m.

TABLE 2. Optimized dimension of antenna B.

Par.	Size (μm)	Par.	Size (μm)	Par.	Size (μm)
L_{SUB}	1350.0	g_1	22.75	$d_{21} = d_{31}$	200.0
W_{SUB}	1000.0	P_{L1}	133.75	W_{11}	130.0
h_{SUB}	60.0	P_{W1}	225.0	L_{11}	75.0
W_{g1}	143.5	d_{11}	265.0	L_{m1}	166.25

It is that for better directive gain exactly along $\phi = 90°$, the radiating and parasitic patches shown in Fig. 2(a) are altered from Antenna A to Antenna C. Table 3 shows the optimized dimensions of Antenna C shown in Fig. 4(a) as given below.

TABLE 3. Optimized dimension of antenna C.

Par.	Size (μm)	Par.	Size (μm)	Par.	Size (μm)
L_{SUB}	1350.0	g_3	15.0	P_3	211.50
W_{SUB}	1000.0	L_{m2}	140.0	d_{21}	232.50
h_{SUB}	60.0	P_1	173.50	d_{22}	200.0
W_{g2}	85.0	P_2	92.50	d_{23}	200.0
W_{21}	100.0	L_{21}	75.0		

Also, a minimal gap (g_3) of 15.0 μm provides better impedance matching. Similarly, the length of the ground is also reduced from 216.50 μm (Antenna A) to 85 μm (Antenna C). The parasitic patch occupies an area of $W_{21} \times L_{21}\ \mu m^2$ with a spacing between them to be d_{21}, d_{22}, and d_{23}, respectively, for better coupling of the signals. Fig. 4(b) displays the comparison of the S_{11} parameter obtained from the two simulators HFSS & CST Microwave Studio.

As per the observations, in both cases required bandwidth for 300 GHz is achieved in addition to good directive gain. This antenna operates between 261 GHz to 387 GHz (HFSS). Moreover, it is observed that the maximum radiation is pointing more toward $\phi = 90°$ than Antenna B and the peak gain noted is 9.14 dBi. In today's wireless world, antennas need to be integrated onto compact, portable, and flexible wireless systems for advanced technologies. Hence, a

TABLE 4. Lumped equivalent component values.

Resistance (Ω)		Inductance (nH)		Capacitance (pF)	
R_1	41.2	L_1	0.023	C_1	0.07
R_2	0.05	L_2	0.02		
R_3	0.05	L_3	0.0098	C_2	0.01
		L_4	4.34565		

TABLE 5. Performance characteristics for different metals.

Material	S_{11} at 300 GHz	Gain (dBi)	Rad. efficiency (%)
Gold	-37.68 dB	8.62	98.38
Chromium	-33.88 dB	8.52	96.31
Platinum	-34.65 dB	8.519	96.63
Titanium	-29.79 dB	8.326	91.59
Tungsten	-36.17 dB	8.562	97.55
Copper	-41.46 dB	8.572	98.61
Aluminium	-40.68 dB	8.553	98.3

TABLE 6. Performance characteristics for metal thickness (t).

t (μm)	S_{11} at 300 GHz	Gain (dBi)
2.5	-28.97 dB	8.55
5	-37.68 dB	8.62
7.5	-49.49 dB	8.54
10	-35.84 dB	8.45
12.5	-30.898 dB	8.51
15	-27.34 dB	8.39

conformal structure as shown in Fig. 5(a) is attempted. This conformal configuration, forming Antenna D as shown in Figs. 5(a)-(c), is bent with an angle of $\phi = 27°$ with respect to the central axis. The structure dimensions are also modified accordingly to obtain the required performance at 300 GHz. A lumped equivalent circuit as shown in Fig. 5(d) is also developed for the proposed structure to study its transmission line model. The equivalent circuit component values are shown in Table 4. This circuit is developed from the concept of the conventional way of modeling a lumped equivalent circuit studied in [22] and [23].

A fair agreement is also noted between the EM simulation (HFSS) and circuit simulation (ADS) as shown in Fig. 5(e). Fig. 5(e) displays the simulation of the antenna for which the S_{11} result is also obtained by using an equivalent circuit model. This result is used and is also plotted in Fig. 5(e) including a comparison with results obtained from HFSS and CST.

It can be observed that the simulated S_{11} results from all three simulators have almost overlapped with the resonant frequency centered at 300 GHz with a good matching of impedance. This antenna operates between 270 to 333 GHz (HFSS). From Figs. 5(f)-(g), it is noted that the antenna shows high gain and directivity. Fig. 5(f) also shows the antenna's maximum radiation at an angle of 90° with a peak gain

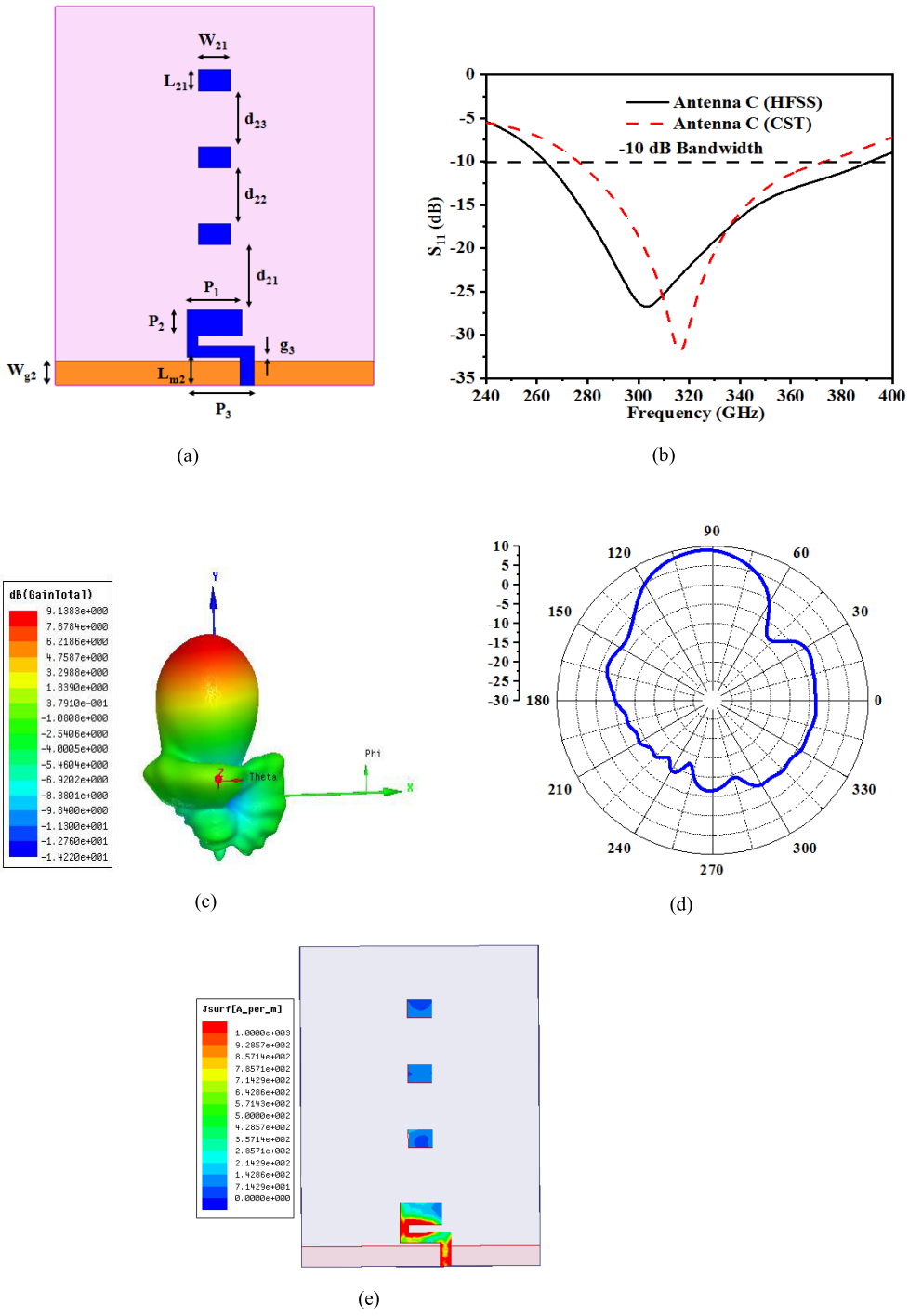

FIGURE 4. Third iteration (Antenna C) (a) Transparent view with optimized dimensions (b) S_{11} (dB) (c)-(e) 3D radiation pattern, XY-plane 2D pattern, surface current distribution at 300 GHz.

of 8.62 dBi. This shows that the maximum radiation is directed toward the end-fire direction with a half-power-beam width (HPBW) of 30°. Fig. 5(h) observes the distribution of surface current density initiated at 300 GHz. The antenna structure connected to the microstrip feed excites the remaining three parasitic elements in the same phase, which leads to an increased gain of the antenna.

III. MATERIAL AND PARAMETRIC VARIATION ON ANTENNA

Fig. 6 shows the parametric variation of key parameters obtained by simulation, which affect the matching of impedance in the operating bandwidth of the proposed antenna. Fig. 6(a) represents the S_{11} graph for different conducting materials including Chromium, Platinum, Gold,

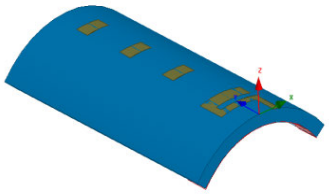

(a)

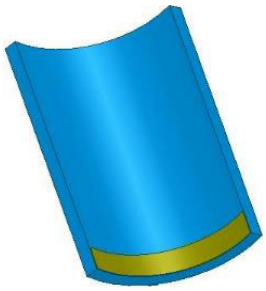

(b)

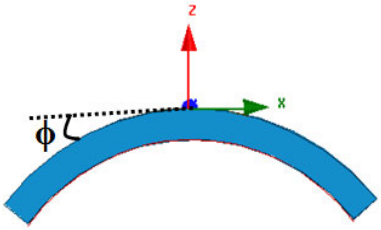

(c)

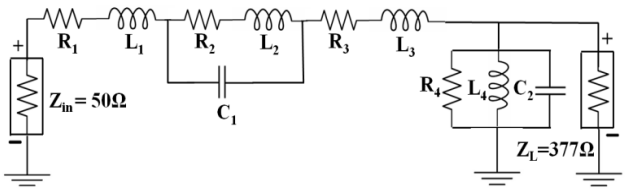

(d)

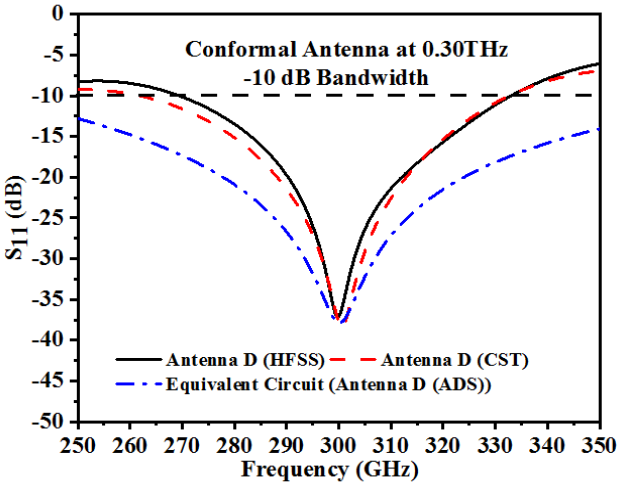

(e)

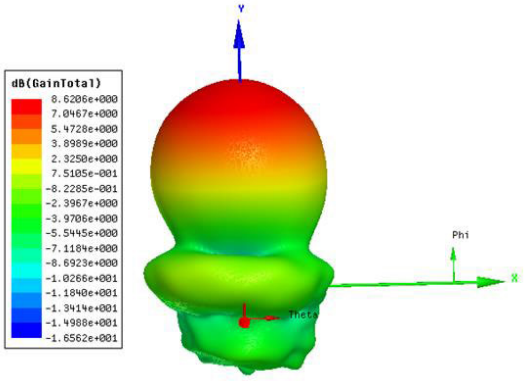

(f)

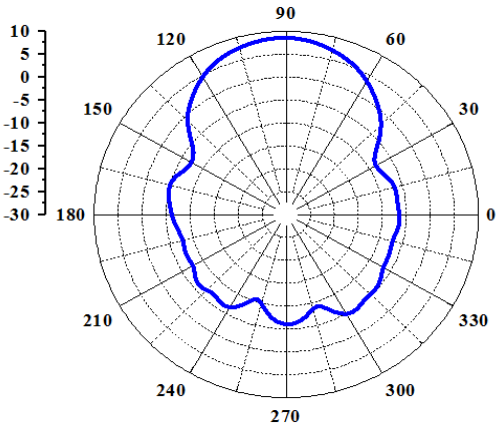

(g)

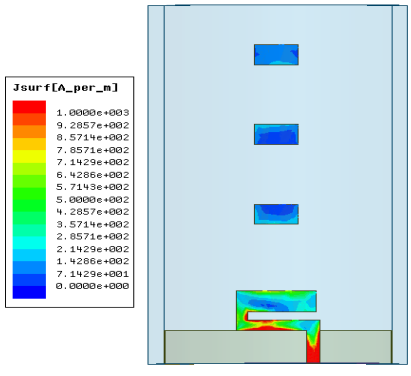

(h)

FIGURE 5. Conformal structure of Antenna D (a)-(c) perspective views (d) Equivalent circuit model (e) S_{11} (dB) (f)-(h) end-fire 3D & 2D radiation pattern, surface current distribution at 300 GHz.

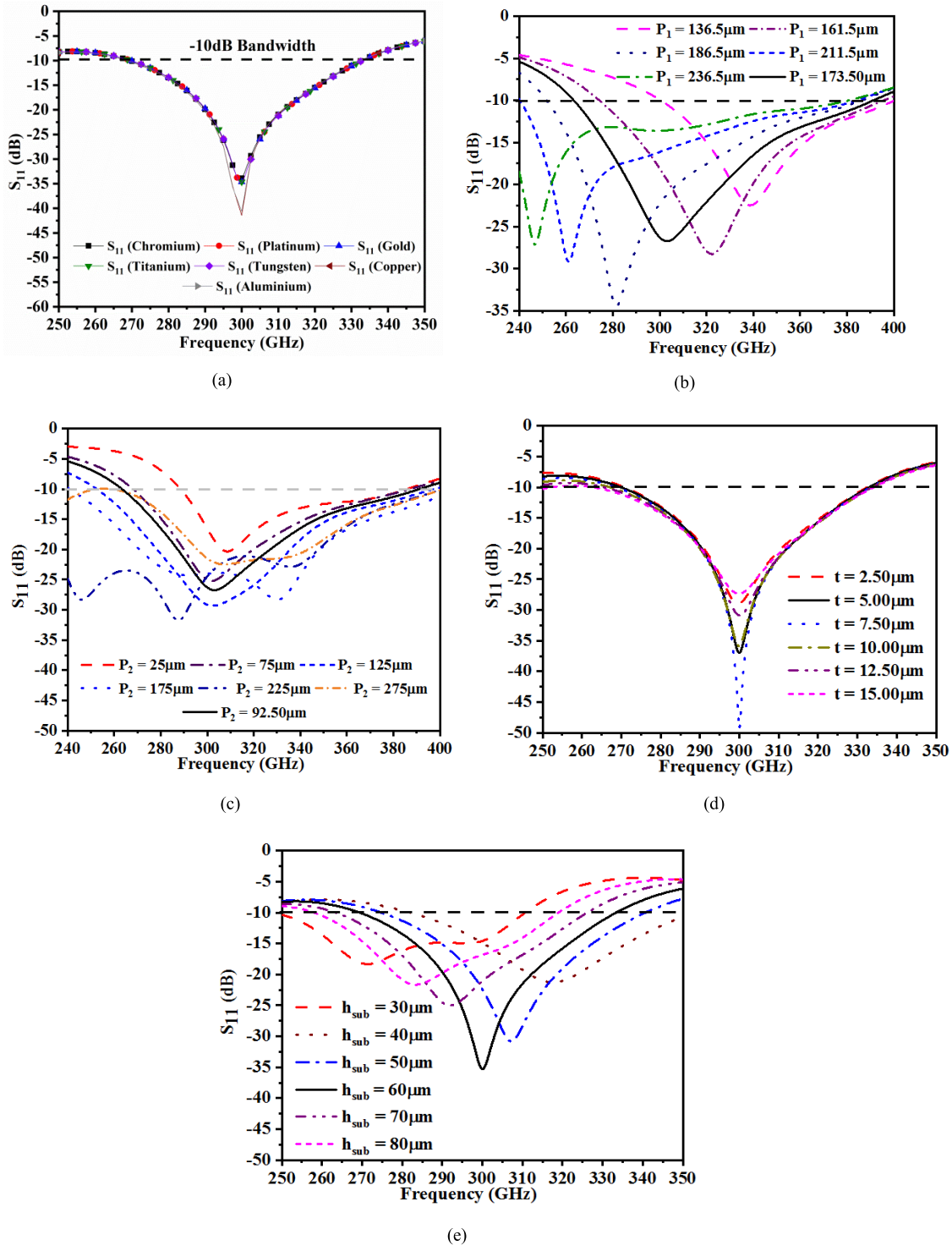

FIGURE 6. (a) The S_{11} parameter for different metals (b)-(e) optimization results in P_1 (width of the patch), P_2 (length of the patch), thickness (t) of gold conducting material, and substrate height (h_{sub}) variation.

Titanium, Copper, Aluminium, and Tungsten. The graph shows that the impedance is matched at 300 GHz for all the above metals. However, in the proposed antenna, Gold is used on the SiO_2 substrate since it provides an excellent radiation pattern and a high gain as shown in Table 5. Fig. 6(b)-(c) shows the parametric variation on the planar patch connected to the microstrip feed line, which also excites the three parasitic elements. The physical length (P_1) is varied from 136.5 μm to 236.5 μm with a step of 25 μm, as shown in Fig. 6(b). For P_1 = 173.50 μm, the antenna resonates at 300 GHz with a bandwidth from 261 GHz to 387 GHz. Fig. 6(c) also shows another physical length (P_2) variation

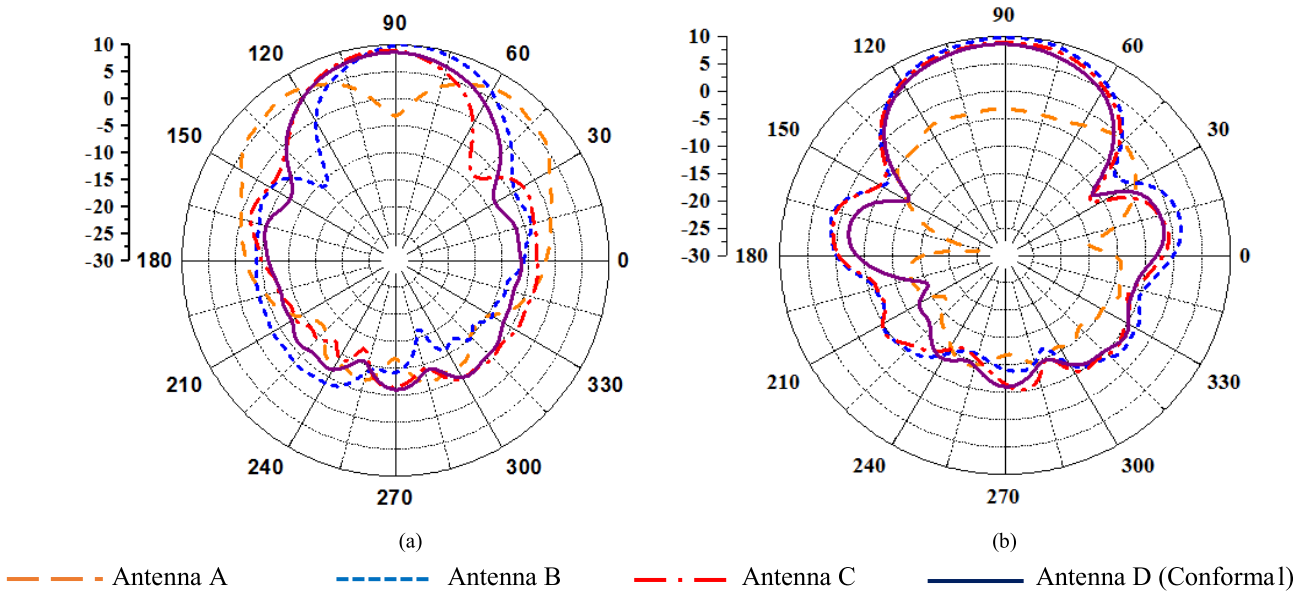

FIGURE 7. 2-D radiation pattern (a) Antenna A to Antenna D in XY-plane (b) Antenna A to Antenna D in YZ-plane.

TABLE 7. Comparison of the proposed conformal antenna with recently published work.

Ref.	Operating band (THz)	Substrate & Permittivity	Size (μm^2)	Peak Gain (dBi)	Terminology Used	Comments on Radiation Patterns	Conformal Capability
[1]	0.88 - 1.62	Rogers RO 3003 $\varepsilon_r = 3.0$	450×950	2.18	Photonic Crystal	80° angle of maximum radiation in E-plane	NO
[3]	0.60 - 1.60	Rogers RO5880 $\varepsilon_r = 2.2$	200×340	7.703	Photonic Crystal	Bi-directional and Omni-directional	NO
[4]	2.00, 3.25, 4.40	Silicon $\varepsilon_r = 11.90$	40×40	-	Graphene Patch	Bi-directional and Omni-directional	NO
[5]	0.274 - 0.296	FR4 $\varepsilon_r = 4.40$	345×423	-	Split-Ring Resonator	Bi-directional and Omni-directional	NO
[9]	0.258 - 0.355	RT6006 $\varepsilon_r = 6.15$	460×1200	5.60	Slots in Patch for Circular Polarization	Radiation pattern with circular polarization	NO
[12]	0.30 - 9.30	Polyamide $\varepsilon_r = 4.30$	600×800	-	Fractal Patch for Super-wideband	Omni-directional in H-plane	NO
[13]	0.683 - 0.711	RO 3003 $\varepsilon_r = 3.0$	180×210	6.793	Photonic Band Gap	Directive radiation Pattern at 0°	NO
[14]	2.42 - 10.52	Polyamide	22×42	5.50	Fractal Patch	Bi-directional and omnidirectional	NO
[15]	1.96 - 2.41	GaAs $\varepsilon_r = 13.0$	60×70	-	Photonic Crystal	Bi-directional and omnidirectional	NO
*P	0.261 - 0.387	Silicon Dioxide $\varepsilon_r = 4.0$	1000×1350 (Antenna C)	9.14	Quasi-Yagi with an Offset Feed	Highly directional in the direction of 90°	YES
	0.270 – 0.333		Antenna D (Conformal)	8.62			

***P - proposed work**

which also plays a major role in achieving resonance at 300 GHz. The patch length (P_2) is varied from 25 to 275 μm resulting in resonance at 300 GHz for $P_2 =$ 92.50 μm, where the objective of this design is achieved with the optimized length. Fig. 6(d) shows the plot of S_{11} for various thicknesses (t) of Gold from 2.50 to 15.00 μm. In all values of t, the resonance value is not changed rather the matching impedance at the resonance frequency (300 GHz) is matched at different real and imaginary impedance values. It is noted that for t = 5.00 μm, the S_{11} corresponds to −37.68 dB at 300 GHz which is the proposed design. Fig. 6(e) presents a variation in substrate height (h_{sub}), which confirms that the resonance at 300 GHz is achieved with a height of 60 μm. A comparison of the performance characteristics for a variation in metals and metal thickness (t) is presented in Tables 5 and 6.

IV. FAR-FIELD RESULT DISCUSSION AND COMPARISON OF PRESENT STATE-OF-THE-ART WITH LITERATURE

Fig. 7 shows the 2-D radiation pattern for all four antennas (Antenna A, Antenna B, Antenna C, and Antenna D) plotted in XY and YZ planes. These radiation patterns are plotted at 300 GHz frequency. For Antenna A and Antenna B, the 2-D radiation patterns in XY and YZ planes show that the wide radiation pattern does not exactly point maximum radiation towards $\phi = 90°$. However, for Antenna C (proposed planar antenna), the radiation pattern becomes more directive toward 90° in both XY and YZ planes. The maximum gain in the end-fire direction corresponds to 9.14 dBi with very low back-lobe radiation. Antenna D, which is the conformal transformation of Antenna C, also corresponds to maximum radiation in the end-fire direction along XY and YZ planes. A peak gain of 8.62 dBi at 300 GHz is noted.

A comparison of the proposed planar antenna (Antenna C) with the literature is performed in Table 7. In the design, three parasitic elements are used as radiating elements along with the main radiating patch which is connected to the offset feed. This is the unique methodology used in designing the proposed antenna. The other THz antennas mentioned in the literature above do not feature a technique for increasing the gain. These antennas also provide bi-directional and omnidirectional 2-D radiation patterns. Since the proposed structure is well-performing, conformal, highly directional, and compact, hence, it can be used in applications such as wearable devices, healthcare applications, etc.

V. CONCLUSION

This work discussed a THz conformal antenna configuration at 300 GHz on a SiO_2 substrate having a thickness of 60 μm and gold as the metal patch and ground. The antenna, with three additional rectangular parasitic patches, is excited by the main patch which is connected to the feed line. The proposed antenna operates from 270 GHz to 333 GHz and offers a high directional behavior in both XY and YZ planes at an angle of 90° having a peak gain of 8.62 dBi. The transmission line equivalent model circuit simulation also presented good coordination with EM simulation. This conformal configuration of the proposed THz antenna is compact and cost-effective. It has high gain, portable, and well-performing. Hence, it can be useful in curved microwave devices such as smartphones, watches, healthcare, etc.

Declaration of Competing Interest

The authors declare that they have no known competing financial interests or personal relationships that could have appeared to influence the work reported in this paper.

REFERENCES

[1] A. Singh and S. Singh, "A trapezoidal microstrip patch antenna on photonic crystal substrate for high speed THz applications," *Photon. Nanostruct. Fundam. Appl.*, vol. 14, pp. 52–62, Apr. 2015.

[2] S. Singhal, "Compact wideband antenna for 60 GHz millimeter wave applications," *Microw. Rev.*, vol. 27, no. 1, pp. 23–27, Jul. 2021.

[3] A. Vahdati and F. Parandin, "Antenna patch design using a photonic crystal substrate at a frequency of 1.6 THz," *Wireless Pers. Commun.*, vol. 109, no. 4, pp. 2213–2219, Dec. 2019.

[4] M. Dashti and J. D. Carey, "Graphene microstrip patch ultrawide band antennas for THz communications," *Adv. Funct. Mater.*, vol. 28, no. 11, Mar. 2018, Art. no. 1705925.

[5] S. Bie and S. Pu, "Array design of 300 GHz dual-band microstrip antenna based on dual-surfaced multiple split-ring resonators," *Sensors*, vol. 21, no. 14, pp. 1–13, Jul. 2021.

[6] V. Semkin, "Beam switching conformal antenna array for mm-wave communications," *IEEE Antennas Wireless Propag. Lett.*, vol. 15, pp. 28–31, 2015.

[7] S. Sengupta, D. R. Jackson, and S. A. Long, "A method for analyzing a linear series-fed rectangular microstrip antenna array," *IEEE Trans. Antennas Propag.*, vol. 63, no. 8, pp. 3731–3736, Aug. 2015.

[8] R. Z. Syeda, "Design and performance analysis of switched beam series-fed patch antenna for 60 GHz WPAN applications," M.S. thesis, Dept. Signal Theory Commun. (TSC), Polytech. Univ. Cataluña (UPC), Barcelona, Spain, 2014, pp. 1–76.

[9] S. Ullah, C. Ruan, M. S. Sadiq, T. U. Haq, and W. He, "Microstrip system on-chip circular polarized (CP) slotted antenna for THz communication application," *J. Electromagn. Waves Appl.*, vol. 34, no. 8, pp. 1029–1038, May 2020.

[10] J. F. O'Hara, S. Ekin, W. Choi, and I. Song, "A perspective on terahertz next-generation wireless communications," *Technologies*, vol. 7, no. 43, pp. 1–18, Jun. 2019.

[11] J. Yan, H. Wang, J. Yin, C. Yu, and W. Hong, "Planar series-fed antenna array for 77 GHz automotive radar," in *Proc. 6th Asia–Pacific Conf. Antennas Propag. (APCAP)*, Oct. 2017, pp. 1–3.

[12] S. Singhal, "Elliptical ring terahertz fractal antenna," *Optik*, vol. 194, Oct. 2019, Art. no. 163129.

[13] S. Ullah, C. Ruan, T. U. Haq, and X. Zhang, "High performance THz patch antenna using photonic band gap and defected ground structure," *J. Electromagn. Waves Appl.*, vol. 33, no. 15, pp. 1943–1954, Oct. 2019.

[14] S. Singhal, "Asymmetrically CPW fed square Sierpinski carpet ultra wideband terahertz antenna," *Optik*, vol. 242, Sep. 2021, Art. no. 167056.

[15] E. C. Britto, S. K. Danasegaran, and W. W. Johnson, "Design of slotted patch antenna based on photonic crystal for wireless communication," *Int. J. Commun. Syst.*, vol. 34, no. 1, pp. 1–11, 2021.

[16] S. Singhal, "Ultrawideband elliptical microstrip antenna for terahertz applications," *Microw. Opt. Technol. Lett.*, vol. 61, no. 10, pp. 2366–2373, Oct. 2019.

[17] S. Singhal, "CPW fed Koch snowflake superwideband terahertz spatial diversity antenna," *Optik*, vol. 206, Mar. 2020, Art. no. 164329.

[18] S. Singhal, "Compact superwideband terahertz antenna," in *Proc. URSI Regional Conf. Radio Sci. (URSI-RCRS)*, Feb. 2020, pp. 1–4.

[19] U. Nissanov, G. Singh, E. Gelbart, and N. Kumar, "Highly directive microstrip array antenna with FSS for future generation cellular communication at THz band," *Wireless Pers. Commun.*, vol. 118, no. 1, pp. 599–617, May 2021.

[20] K. R. Jha and G. Singh, "Terahertz planar antennas for future wireless communication: A technical review," *Infr. Phys. Technol.*, vol. 60, pp. 71–80, Sep. 2013.

[21] B. Aqlan, M. Himdi, H. Vettikalladi, and L. Le-Coq, "A 300-GHz low-cost high-gain fully metallic Fabry–Pérot cavity antenna for 6G terahertz wireless communications," *Sci. Rep.*, vol. 11, no. 1, p. 7703, Apr. 2021.
[22] N. Anveshkumar and A. S. Gandhi, "Lumped equivalent models of narrowband antennas and isolation enhancement in a three antennas system," *Radioengineering*, vol. 27, no. 3, pp. 646–653, Sep. 2018.
[23] A. Nella and A. Gandhi, "Typical approach of modeling lumped equivalents for narrowband antennas," *Int. J. Microw. Opt. Technol.*, vol. 14, no. 5, pp. 298–305, 2019.
[24] S. Das, D. Mitra, and S. R. B. Chaudhuri, "Fractal loaded planar super wide band four element MIMO antenna for THz applications," *Nano Commun. Netw.*, vol. 30, Dec. 2021, Art. no. 100374.
[25] G. Varshney, S. Gotra, V. S. Pandey, and R. S. Yaduvanshi, "Proximity-coupled two-port multi-input-multi-output graphene antenna with pattern diversity for THz applications," *Nano Commun. Netw.*, vol. 21, Sep. 2019, Art. no. 100246.
[26] A. Mohanty and S. Sahu, "A micro 4-port THz MIMO antenna for nano communication networks," *Photon. Nanostruct.-Fundam. Appl.*, vol. 53, pp. 1–14, 2023.
[27] N. K. Maurya, S. Kumari, P. Pareek, and L. Singh, "Graphene-based frequency agile isolation enhancement mechanism for MIMO antenna in terahertz regime," *Int. J. Electron. Commun.*, vol. 35, pp. 1–18, Jan. 2023.
[28] K. Muthukrishnan, M. M. Kamruzzaman, S. Lavadiya, and V. Sorathiya, "Superlative split ring resonator shaped ultrawideband and high gain 1×2 MIMO antenna array for Terahertz Communication," *Int. J. Electron. Commun.*, vol. 33, pp. 1–18, Jun. 2023.

ANVESHKUMAR NELLA (Member, IEEE) received the Ph.D. degree from the Department of Electronics and Communications Engineering, VNIT, Nagpur, India, in 2019.

He is currently an Assistant Professor with the School of Electrical and Electronic Engineering, VIT Bhopal University, Bhopal, Madhya Pradesh, India. He is also having four years of teaching and research experience. He has published his research and review articles 18 in SCI/SCIE, three in Scopus, five in international/national journals, and 16 in international/national conferences. He has edited three textbooks published by Springer, in 2021 and 2022. He is also a Co-PI and a research consultant for several funded projects. His research interests include antennas, RF circuits, and wireless communications. He is also working in the areas of plasmonic absorbers, meta-materials, high-directional UWB antennas, reconfigurable antennas, cognitive radio antennas, RF energy harvesting, and THz and mobile antennas. He is a regular reviewer of various IEEE, IET, Elsevier, Springer, Wiley, and MDPI journals.

VIGNESWARAN DHASARATHAN received the Ph.D. degree in information and communication engineering and the specific areas of research include optical communication, photonic networks, and wireless optical communication in the higher end of the 5G networks.

He is currently working with space division multiplexing applications for avoiding the cross-talk effects of dense network optical systems, and also working as a Research Scientist at the University of Hradec Králové, Czech Republic. In addition, he is also working in the fields of photonics 2D materials, photonics sensing, nonlinear photonics, UWB antenna, and flexible antenna. He also moves his career as a Research Consultant with Ton Duc Thang University, Vietnam. He has published around 60 articles in well-reputed journals, including, IEEE, Nature, Springer, Wiley, SPIE, world scientific publisher, Taylor Francis, IET, and OSA. As a reviewer, he has reviewed more than 100 articles from various journals, including IEEE, Nature, and OSA. He was declared as a fastest and reviewer appreciation from Elsevier and Springer. He is also in one of the reputed editor panel members and serves as an Associate Editor for the *Wireless Network* (Springer) and *Network Modeling Analysis in Health Informatics and Bioinformatics* (Springer).

JAN KŘÍŽ received the Ph.D. degree in theoretical physics from the Faculty of Mathematics and Physics, Charles University, Prague, in 2003.

Since 2019, he has been the Dean of the Faculty of Science, University of Hradec Králové, Czech Republic. His research interests include the mathematical physics of quantum systems, deformed quantum mechanics, data processing techniques, and creating physics tasks for talented pupils.

TATHABABU ADDEPALLI received the B.Tech. degree from JNTUH, Hyderabad, in 2007, the M.Tech. degree from JNTUK, Kakinada, in 2010, and the Ph.D. degree from JNTUA, Anantapur, in 2022.

He has published ten SCIE research articles in various reputed international journals in Elsevier, Wiley, MDPI Springer, and Taylor & Francis. He has also presented five conferences (four IEEE and one Springer) and published two book chapters on THz and planar antennas. He attended more than 40 workshops in various reputed institutions. His research interests include microstrip patch antennas, MIMO antennas, 5G antennas, flexible antennas, characteristic mode analysis (CMA), THz antennas, and metamaterial antennas.

ŠTĚPÁN HUBÁLOVSKÝ received the M.Sc. and Ph.D. degrees from the Faculty of Mathematics and Physics, Charles University, Prague, Czech Republic, in 1995 and 1998, respectively. He became an Associate Professor with the Faculty of Informatics and Management, University of Hradec Kralove, Czech Republic, in 2012, where he is currently the Vice Dean of the Faculty of Science. His research interests include technical cybernetics, computer simulation, and optimization and data processing.

MANISH SHARMA (Senior Member, IEEE) received the B.E. degree in electronics and communication engineering from Mangalore University, Karnataka, India, in 2000, the M.Tech. degree from Visvesvaraya Technological University, Karnataka, in 2007, and the Ph.D. degree from the Department of Electronics Engineering, Banasthali University, Rajasthan, India, in 2017. He is currently a Professor/a Researcher with Chitkara University Research and Innovation Network (CURIN), Chitkara University, Punjab, India. He has published more than 100 research articles and granted with eight patents. He is also guiding eight Ph.D. students. He has also published 18 book chapters. His research interests include computational electromagnetics, reconfigurable antennas, novel electromagnetic materials, dielectric resonator antennas, wideband/superwideband antennas, wideband/dual band/triple band microstrip antennas for wireless communication, smart and MIMO antennas systems, radio-frequency identification (RFID) antennas, antennas for healthcare, RF MEMS planar antenna on Si substrate, wireless networks, body area networks, meta surface-based biosensors, and designing of microstrip antennas using machine learning and artificial networks. He is a reviewer of IEEE Access, *Journal of Electromagnetic Waves and Applications*, *International Journal of Electronics and Communication* (AEU), *International Journal of Communication Systems*, *International Journal of Microwave and Wireless Technologies*, and *International Journal of RF and Microwave Computer-Aided Engineering*.